# Mechanism of inhibition of delayed rectifier $K^+$ current by 4-aminopyridine in rabbit coronary myocytes

C. V. Remillard and N. Leblanc*

*Département de Physiologie, Université de Montréal and Centre de Recherche, Institut de Cardiologie de Montréal, Montréal, QC, Canada H1T 1C8*

1. The mechanisms involved in the 4-aminopyridine (4-AP)-induced block of delayed rectifier $K^+$ current ($I_{K(V)}$) in vascular smooth muscle cells were studied in cells enzymatically isolated from the rabbit coronary artery.

2. 4-AP inhibited slowly inactivating $I_{K(V)}$ in a dose-dependent manner (concentration producing half-maximal inhibition, $K_{½}$, = 1·37 mM), and shifted the steady-state activation and inactivation curves of $I_{K(V)}$ by +9 and +16 mV, respectively.

3. The time constant of activation was significantly increased by 4-AP at +20 mV; deactivation kinetics were unaffected upon repolarization to −40 mV. The fast ($\tau_f \approx 1$ s) and slow ($\tau_s \approx 5$ s) time constants of inactivation (0 and +20 mV), and the recovery kinetics ($\tau_r \approx 6$ s) at −60 mV were not significantly affected by 0·5 mM 4-AP. However, $\tau_f$ disappeared in the presence of 2 mM 4-AP while $\tau_s$ remained unaffected.

4. Use-dependent unblock of $I_{K(V)}$ was revealed at potentials $\geqslant -10$ mV from analyses of the voltage dependence of 4-AP-sensitive currents and the frequency-dependent changes ('reverse use dependence') of $I_{K(V)}$ during the application of repetitive steps (−60 to +20 mV for 250 ms at a rate of 0·25 Hz) in control conditions, in the presence of 0·5 mM 4-AP, and after washout of the drug. These results suggested that 4-AP preferentially binds to the channel in the closed state, and unbinding is promoted by transitions to the open state.

5. The channel was modelled as a simple three-state mathematical loop model incorporating single closed, open and inactivated states. The block by 4-AP was modelled as a state-dependent interaction with 4-AP primarily binding to the closed state. Computer simulations support the hypothesis that 4-AP-induced block of the delayed rectifier $K^+$ ($K_V$) channel in the closed state is relieved during membrane depolarization.

6. Closed state binding of 4-AP to the $K_V$ channel depolarizes vascular smooth muscle cells by shifting the activation curve of these channels to more positive potentials.

A voltage-dependent delayed rectifier $K^+$ ($K_V$) channel has been identified, and its properties studied, in various types of smooth muscle cells. Its importance in determining resting membrane potential ($E_m$) has been well characterized in coronary artery (Leblanc, Wan & Leung, 1994), trachea (Boyle, Tomasic & Kotlikoff, 1992; Fleischmann, Washabau & Kotlikoff, 1993) portal vein (Miller, Morales, Leblanc & Cole, 1993), and pulmonary artery smooth muscle cells (Okabe, Kitamura & Kuriyama, 1987; Post, Hume, Archer & Weir, 1992; Smirnov, Robertson, Ward & Aaronson, 1994; Yuan, Tod, Rubin & Blaustein, 1994). These studies agree that the delayed rectifier $K^+$ current ($I_{K(V)}$) represents the dominant repolarizing conductance within the physiological range of membrane potentials (−50 to 0 mV) and is critical in determining $E_m$ at low or normal intracellular $Ca^{2+}$ levels ($[Ca^{2+}]_i$). The single-channel correlate of $I_{K(V)}$ exhibits a conductance in the range of 5–57 pS, is voltage dependent, displays activation and inactivation kinetics, is blocked by intracellular $Mg^{2+}$ or $Ca^{2+}$ (Gelband & Hume, 1992), and is blocked by 4-aminopyridine (4-AP), while being relatively insensitive to tetraethylammonium chloride or charybdotoxin, which have been widely used to inhibit large-conductance potassium channels (Beech & Bolton, 1989*b*; Volk, Matsuda & Shibata, 1991; Brayden & Nelson, 1992; Gelband & Hume, 1992; Volk & Shibata, 1993; Miller *et al.* 1993; Leblanc *et al.* 1994). Recently, the inhibition of $I_{K(V)}$ has been suggested to play a direct role in causing acute (Post *et al.* 1992; Yuan *et al.* 1994) as well as chronic (Smirnov *et al.* 1994) hypoxic pulmonary vasoconstriction.

* To whom correspondence should be addressed.

The use of 4-aminopyridine as a specific blocker of $I_{K(V)}$ has been crucial in assessing its physiological function in smooth muscle. Although $Ca^{2+}$-activated $K^+$ channels were shown to be insensitive to 4-AP (Beech & Bolton, 1989*b*; Boyle *et al.* 1992; Gelband & Hume, 1992; Miller *et al.* 1993; Leblanc *et al.* 1994), the compound has also been shown to block the '$I_A$-type' of transient outward $K^+$ current in smooth muscle cells ($I_{to}$) (Beech & Bolton, 1989*a*; Vogalis & Lang, 1994). However, $I_{to}$ represented a relatively small fraction of total outward current in rabbit portal vein cells (Beech & Bolton, 1989*a*). In addition, the channel was reported to be largely inactivated at physiological membrane potentials recorded in vascular (Beech & Bolton, 1989*a*) and colonic (Vogalis & Lang, 1994) smooth muscle cells. Thus, under well-defined conditions, 4-AP appears to be a useful tool to investigate the role of $K_V$ channels in vascular smooth muscle cells.

Despite extensive use of 4-AP to separate pharmacologically the different $K^+$ channels participating in total macroscopic current, few studies have elucidated the mechanisms involved in the inhibition of the $K_V$ channel in smooth muscle cells. To date, a few suggested mechanisms have surfaced: (i) 4-AP decreases the open probability of the channel, with no effect on the amplitude of single-channel unitary currents (Boyle *et al.* 1992; Russell *et al.* 1994*b*); (ii) either ionized or non-ionized, 4-AP permeates the membrane to bind the channel from the inside (Okabe *et al.* 1987); and (iii) 4-AP appears less potent at inhibiting $I_{K(V)}$ at more positive potentials, suggesting a reduced action on channels in the open state (Okabe *et al.* 1987; Volk *et al.* 1991; Gelband & Hume, 1992; Leblanc *et al.* 1994; Robertson & Nelson, 1994). We have previously reported that unblock of 4-AP from the $K_V$ channel might be occurring in rabbit coronary myocytes; this is based on the analysis of a 4-AP-sensitive current evoked during ramp or step protocols (Leblanc *et al.* 1994). The major aim of this study was to investigate in further detail the mechanisms by which 4-AP blocks delayed rectifier $K^+$ currents in whole-cell voltage-clamped rabbit coronary myocytes.

Our data show that 4-AP preferentially binds to the $K_V$ channel in the closed state and unbinds during membrane depolarization-induced channel activation. Closed state binding of 4-AP to $K_V$ channels depolarizes vascular smooth muscle cells by shifting the activation curve of these channels to more positive potentials. This work has been presented in preliminary form (Remillard & Leblanc, 1995).

## METHODS

### Cell isolation procedure

This study was approved by the ethical and animal care committees of the Montreal Heart Institute (Montreal, Canada). Isolation of single coronary smooth muscle cells was performed using an enzymatic dispersion method. Briefly, albino rabbits (1·5–2·0 kg) of either sex were killed by cervical dislocation late in the day. The heart was quickly removed and placed in a cold and well-oxygenated (95% $O_2$–5% $CO_2$) 10 $\mu$M $Ca^{2+}$ dissection solution containing (mM): NaCl, 120; $NaHCO_3$, 25; KCl, 4·2; $KH_2PO_4$, 1·2; $MgCl_2$, 1·2; glucose, 11; taurine, 25; adenosine, 0·02 (taurine and adenosine from Sigma); and $CaCl_2$, 0·01. The left anterior descending and the circumflex coronary arteries were carefully removed from the ventricular muscle and pinned onto a silicone elastomer-filled Petri dish (Sylgard 184; Dow Corning Co., Midland, MI, USA). All adhering ventricular myocardium and connective tissue were carefully removed from the arteries under binocular examination. Both vessels were then placed in individual tubes for enzymatic dispersion. The composition of the enzyme solution was as follows (per millilitre of 10 $\mu$M $Ca^{2+}$ dissecting solution): 0·6 mg of collagenase Type 1A (320 units $mg^{-1}$; Sigma); 0·2 mg of trypsin inhibitor (Sigma); 50 $\mu$l of protease Type XXVII (1 mg $ml^{-1}$ stock; Sigma). The arteries were left overnight in the enzyme solution at 4 °C for a maximum of 16 h. After digestion, the arteries were retrieved and rinsed several times with fresh 10 $\mu$M $Ca^{2+}$ solution, placed in a bovine serum albumin solution (1 mg $ml^{-1}$ of 10 $\mu$M $Ca^{2+}$ solution; Sigma) and incubated at 35 °C for 2 min. Single smooth muscle cells were mechanically dispersed by triturating the tissues in 10 $\mu$M $Ca^{2+}$ solution. All tissues and supernatant containing single cells were stored at 4 °C until use. Data were acquired within 4–8 h of cell isolation.

### Experimental procedure and electrophysiological techniques

All experiments were performed at room temperature (21–23 °C) using either of two inverted microscopes: Nikon Diaphot model TMD, or Nikon model TMS (Nikon Corp., Tokyo, Japan). The recording chamber (volume ≈ 1 ml) was mounted on a moveable stage and cleaned thoroughly with 95% ethanol before use. Before each experiment, a sample of the supernatant containing single cells was deposited in the experimental chamber and the cells were allowed to settle for 30 min. Patch-clamp experiments were carried out only on cells which remained in a relaxed state following the initial superperfusion with the normal Hepes–bicarbonate solution used in the experiments (see composition below).

The standard whole-cell configuration of the patch-clamp technique was used to voltage-clamp single coronary artery smooth muscle cells (Hamill, Marty, Neher, Sakmann & Sigworth, 1981). Borosilicate patch micropipettes were pulled on a two-stage vertical puller (model PP-83; Narashige Scientific Instruments Laboratories, Tokyo, Japan) and heat polished using a microforge (model MF-83; Narashige Scientific Instruments Laboratories). The micropipette diameter was 1–2 $\mu$m. Pipette resistance ranged from 4 to 6 MΩ when the pipette was filled with internal solution (see below for description).

The pipette tip was brought towards a single coronary artery smooth muscle cell using a motorized micromanipulator (Fine Science Tools Inc., North Vancouver, BC, Canada) driven by a control unit (model MS-314; Fine Science Tools Inc.). A membrane–pipette gigaohm seal (2–10 GΩ) was established by applying gentle pressure to the cell, followed by negative pressure via a syringe attached to the micropipette holder. Intracellular access was then obtained by applying more suction. Series resistance compensation was performed in all experiments.

The signal recorded from the micropipette was transmitted to the headstage (50 MΩ feedback resistor) of a patch-clamp amplifier (model Axopatch-1D; Axon Instruments Inc., Burlingame, CA, USA). Voltage-clamp protocols, data acquisition and analysis were performed with a computer (IBM AT-486 compatible) using the pCLAMP software (Version 5.5.1; Axon Instruments Inc.). All

data were temporarily stored on the computer hard disk for later analysis. Current and voltage traces were displayed using a Hewlett Packard LaserJet printer (model Series III; Hewlett Packard Co., Mountain View, CA, USA).

### Solutions and drugs

The standard micropipette solution contained (mM): potassium gluconate, 110; KCl, 30; $MgCl_2$, 0·5; Hepes, 5; NaCl, 10; and ATP-Mg, 1 (pH adjusted to 7·2 with KOH). EGTA (5 mM) was added to the solution to buffer intracellular $Ca^{2+}$.

The standard external solution (normal) had the following composition (mM): NaCl, 130; $NaHCO_3$, 10; KCl, 4·2; $KH_2PO_4$, 1·2; $MgCl_2$, 0·5; $CaCl_2$, 1·8; Hepes, 10; glucose, 5·5; nifedipine (10 mM stock in DMSO; Sigma), 0·001 (pH adjusted to 7·35 with NaOH). 4-Aminopyridine (Sigma) was added in powder form at the desired final concentration to the normal external solution and pH readjusted to 7·35 before proceeding.

### Statistical and computational analyses

The values in most graphs are expressed as means ± S.E.M. of $N$ cells, unless the results of a single experiment are represented. Where applicable, Student's paired $t$ test was employed to assess statistical significance of the differences between control and test solutions. A probability of $P \leq 0·05$ was accepted as the level of significance.

Theoretical simulations of the 4-AP-induced block of delayed rectifier $K^+$ current were performed on a 486SL IBM PS/Note portable computer (25 MHz) using the AXON ENGINEER software (Axon Software, Madison, WI, USA). Ordinary differential equations were simultaneously solved by the Gear numerical integration method using 10 ms incremental time steps. All simulations in the absence or presence of 4-AP were initiated in the steady state. Results of the simulations were exported to ASCII files to be processed later by graphics software.

## RESULTS

In these experiments, the activity of $Ca^{2+}$-activated $K^+$ ($K_{Ca}$) and $Cl^-$ ($Cl_{Ca}$) channels was minimized by using 5 mM EGTA in the pipette solution to buffer intracellular $Ca^{2+}$ and, in some experiments, by superfusing the cells with 0·5 mM TEA (Figs 2 and 3). Adenosine triphosphate-sensitive $K^+$ ($K_{ATP}$) channels were inhibited by cell dialysis with 1 mM ATP. L-type $Ca^{2+}$ channels were suppressed by 1 μM nifedipine.

### 4-AP inhibits $I_{K(V)}$ in a dose-dependent fashion

The first series of experiments was done to test the effectiveness of different 4-AP concentrations on $I_{K(V)}$ in our preparation. Figure 1*A* shows a sample experiment in which the effects of two concentrations of 4-AP were tested on $I_{K(V)}$ recorded in one myocyte. Membrane currents were elicited by 20 s steps to +20 mV from holding potential ($V_h$) of −60 mV at 60 s intervals. Figure 1*A a* shows selected traces in control conditions (*i*) and after steady-state

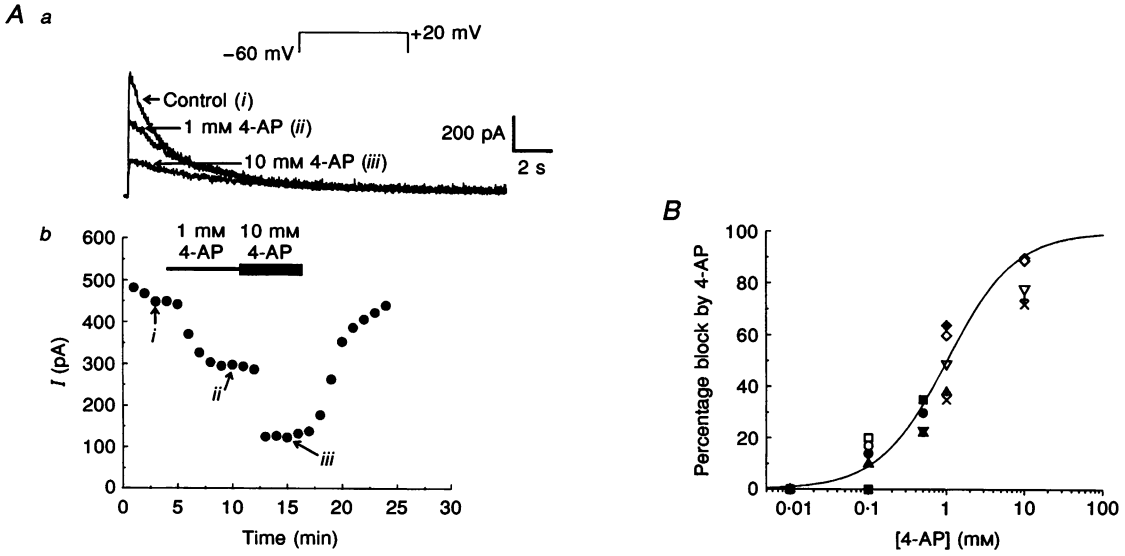


**Figure 1. Concentration-dependent inhibition of $I_{K(V)}$ by 4-AP**

*A*, sample experiment showing the effects of 1 and 10 mM 4-AP on $I_{K(V)}$. Pulse protocol is shown at the top and is described in the text. *A a*, selected traces are shown for control (*i*), 1 mM 4-AP (*ii*) and 10 mM 4-AP (*iii*) conditions. *A b* shows a plot of the time course of changes of $I_{K(V)}$ during the application (bars above data points) and washout of 4-AP. Current magnitude was measured by subtracting the current level at the end of the pulse from peak current. Data points labelled *i*, *ii* and *iii* correspond to measurements carried out on traces displayed in panel *A a*. *B*, dose–response curve of 4-AP on $I_{K(V)}$. Data are results from 12 cells, each cell being represented by a different symbol. A minimum of 5 cells is shown for each concentration. The points were fitted by a power logistic function described by the following equation: $Y=(I_{min} - I_{max})/\{[1 + ([4\text{-AP}]/K_{½})^p] + I_{min}\}$, where $I_{min}$ and $I_{max}$ represent normalized minimal and maximal currents, and $p$ and $K_{½}$ represent, respectively, the slope factor and concentration of 4-AP producing half-maximal inhibition of $I_{K(V)}$. In our experiments, $p$ and $K_{½}$ were 0·705 and 1·37 mM, respectively.

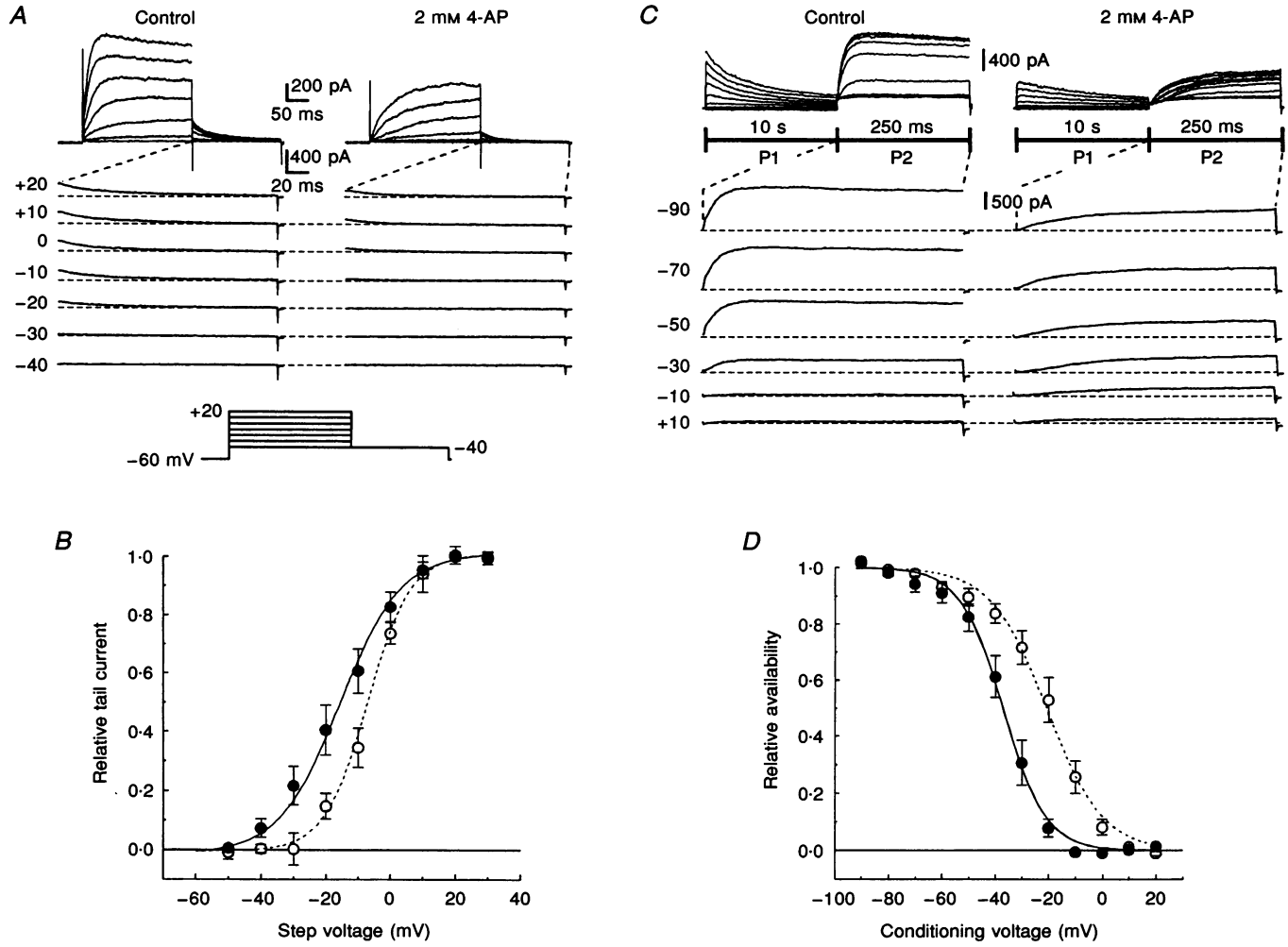


**Figure 2. 4-AP produces a positive shift of the steady-state activation and inactivation curves of $I_{K(V)}$**

*A*, cells were subjected to a standard double-pulse protocol as shown at the bottom of *A*. Traces at top left were elicited by pulsing from −40 to +20 mV in 10 mV increments from a $V_h$ of −60 mV in control conditions. Tail currents evoked upon repolarization to −40 mV are shown at bottom left. Note that tail currents were apparent at −30 mV and reached a maximum level at +20 mV in control conditions (N.B. scales for top and bottom traces are different). Traces at top right show the effects of 2 mM 4-AP on currents evoked by an identical protocol. Representative tail currents are shown at bottom right. Tail currents became apparent only at −10 mV and saturated at potentials > +20 mV. *B*, effects of 4-AP on the steady-state activation curve of $I_{K(V)}$. Protocols used to generate the curves were similar to that described in *A*. Relative states of activation at each voltage and their fits are shown for control conditions (●, continuous line) and in the presence of 2 mM 4-AP (○, dashed line). Values are mean normalized tail currents ± S.E.M. of 10 and 6 cells in control conditions and 4-AP, respectively. Points were fitted using the following form of the Boltzmann equation: $Y = \{1 + \exp[(V_{½} - V)/k]\}^{-1}$, where $V_{½}$ represents half-maximal activation potential and $k$ is the slope factor. $V_{½}$ was −16 and −7 mV in control and 4-AP, respectively; $k$ was 9·4 and 6·7 mV in control and 4-AP, respectively. *C*, current traces were generated using a double-pulse protocol as described in the text. Traces were digitized using a two-clock acquisition protocol. The first 10 s (preconditioning pulses or P1) and last 250 ms (test pulse or P2) were acquired at respective sampling rates of 100 Hz and 4 kHz. Traces obtained in control conditions (top left) and after steady-state block by 2 mM 4-AP (top right) are shown. Reproductions of current traces obtained during the second pulse for selected preconditioning steps are shown below for controls (bottom left) and 4-AP (bottom right). *D*, steady-state inactivation curves were constructed from control (●, continuous line) and 2 mM 4-AP (○, dashed line) measurements. Each data point is a mean ± S.E.M. of $I/I_{max}$ during P2 of 11 and 8 cells in control conditions and 4-AP, respectively. The curves were described by the following form of the Boltzmann equation: $Y = [1 + \exp[(V - V_{½})/k]\}^{-1}$. $V_{½}$ was −37 and −21 mV in control conditions and 4-AP, respectively; $k$ was 8·0 and 10·4 mV in controls and 4-AP, respectively.

inhibition of $I_{K(V)}$ by 1 mM (*ii*) and 10 mM (*iii*) 4-AP. Figure 1*A b* displays the time course of changes in $I_{K(V)}$ during the application of 4-AP and during washout. The traces are labelled as in Fig. 1*A a*. $I_{K(V)}$ was measured by subtracting end from peak current during the step. 4-Aminopyridine inhibited $I_{K(V)}$ in a dose-dependent manner and the inhibition was almost completely reversible upon washout. Experiments such as the one described in Fig. 1*A* served to construct the dose–response relationship of inhibition of $I_{K(V)}$ by 4-AP as summarized in Fig. 1*B*. It was not possible to test all five concentrations of 4-AP (0·01, 0·1, 0·5, 1 and 10 mM) in the same cell; we were able to test at most three concentrations in some cells. These results show that 4-AP inhibited coronary smooth muscle $I_{K(V)}$ with a concentration for half-maximal inhibition ($K_{½}$) of 1·37 mM.

### 4-AP affects steady-state activation and inactivation of $I_{K(V)}$

We first examined whether 4-AP affected $I_{K(V)}$ by shifting the steady-state activation curve. A standard double-pulse protocol was used to estimate the voltage dependence of $I_{K(V)}$ by tail current analysis in the presence and absence of 2 mM 4-AP. The top families of traces shown in Fig. 2*A* were evoked in response to 250 ms steps from −40 to +20 mV from a $V_h$ of −60 mV, as depicted by the protocol shown at the bottom. Tail currents recorded upon repolarization to −40 mV for each voltage step are reproduced below the traces. In control conditions, tail currents became apparent at potentials $\geqslant -30$ mV and increased to reach a maximum near +20 mV. In the presence of 2 mM 4-AP, tail currents were undetectable below −10 mV and increased for step potentials more positive than −20 mV, though it was apparent that their amplitude had still not reached a plateau near +20 mV, as observed in the absence of drug.

Figure 2*B* depicts the effects of 2 mM 4-AP on the steady-state activation curve of $I_{K(V)}$. These curves were constructed using protocols similar to that shown in Fig. 2*A*. Two hundred and fifty millisecond steps were applied in 10 mV increments ranging from either −50 or −40 mV, depending on the magnitude of time-dependent current in individual cells. The initial step which activated $I_{K(V)}$ was followed by a constant 200 ms step to either −40 or −50 mV to record tail current. Steady-state activation curves were generated by plotting normalized tail current amplitude as a function of step potential for each condition. The graph shows that 2 mM 4-AP produced a significant positive shift of the steady-state activation curve of $I_{K(V)}$. Half-maximal activation was shifted by +9 mV in the presence of 4-AP; the voltage dependence was also steepened in the presence of the blocker.

We then verified whether 4-AP influenced the relative availability of $I_{K(V)}$. A standard double-pulse protocol was used to examine the effects of 4-AP on the steady-state inactivation. Figure 2*C* shows a representative experiment in which we have tested the effects of 2 mM 4-AP. The protocol used was similar to that reported by our group (Leblanc *et al.* 1994). Ten second preconditioning steps ranging from −90 to +20 mV were applied in 10 mV increments from a holding potential of −60 mV. Each preconditioning pulse was followed by a constant 250 ms test pulse to +20 mV to record $I_{K(V)}$. Two families of current traces obtained in control conditions (left) and after steady-state block by 2 mM 4-AP (right) are shown at the top of this panel. $I_{K(V)}$ recorded during the second step for selected preconditioning steps (labelled) are reproduced below for comparison. It can be appreciated that, while $I_{K(V)}$ was completely inactivated at potentials $\geqslant -10$ mV in control conditions, a significant fraction of $I_{K(V)}$ remained available at potentials more positive than +10 mV after application of 4-AP.

Figure 2*D* displays the summarized data showing means ± S.E.M. of relative state of availability in control conditions (●) and in the presence of 2 mM 4-AP (○). The continuous and dotted lines are least-squares Boltzmann fits to the mean values illustrated. 4-Aminopyridine produced a +16 mV shift of half-maximal inactivation while having little, if any, effect on the slope of the relationship. The results reported in Fig. 2 suggest that 4-AP has a profound influence on the voltage-dependent mechanisms of gating of the $K_V$ channel in the steady state.

### Effects of 4-AP on kinetics

Since 4-AP appears to interfere with the mechanisms of gating of the $K_V$ channel, it is likely to have some effect on kinetics. Figure 2*A* clearly shows that the onset of activation of the current elicited by short depolarizations was lengthened in the presence of 4-AP. Figure 3 shows the results of analyses of activation and deactivation kinetics. Figure 3*A* displays original current traces obtained in control conditions (larger current) and after steady-state block by 2 mM 4-AP. These currents were evoked by 250 ms steps to +20 mV from a $V_h$ of −60 mV; the membrane was then repolarized for 200 ms to −40 mV to record tail current. The duration of the step to +20 mV was chosen to minimize time-dependent inactivation, although some inactivation was evident in control conditions. For both controls and 4-AP, channel activation and deactivation at +20 and −40 mV, respectively, were reasonably well fitted by monoexponential functions (lines superimposed on the traces with their respective time constants as indicated). In this cell, 4-AP induced a 2·7-fold increase in the time constant of activation at +20 mV; in contrast, deactivation of $I_{K(V)}$ in the presence of 4-AP was similar to that measured in control conditions, with a small tendency for $\tau$ to be smaller with 4-AP.

Figure 3*B* presents a summary of similar data obtained in seven cells. Although the time constant of activation was enhanced by 3·9-fold on average, the time constant of deactivation was not statistically different in 4-AP-treated

*versus* control cells, although a small difference was apparent which was just at the limit of significance ($P = 0{\cdot}076$).

The effects of 4-AP on the kinetics of inactivation and recovery from inactivation were also examined and the results reported in Fig. 4. Figure 4*A* shows typical current traces obtained in control conditions (■) and in the presence of 4-AP (●) at two different step potentials (10 s in duration; $V_h = -60$ mV). Superimposed on each trace are double-exponential (control) and monoexponential (4-AP) fits to the data. The results of such an analysis are reported in Fig. 4*B*. The fast component of inactivation observed in control conditions ($\tau_f$; □) was no longer detectable in the presence of 2 mM 4-AP at either potential. In contrast, the slow time constant of inactivation ($\tau_s$; ■ and ▨) was not significantly affected by 4-AP. With 0·5 mM 4-AP (right set of bars), both $\tau_f$ and $\tau_s$ were apparent at +20 mV and were not significantly modified.

Figure 4*C* shows a representative experiment in which we have tested the effects of 0·5 mM 4-AP on the recovery from inactivation of $I_{K(V)}$. A double-pulse protocol was employed, which consisted of an initial 20 s pulse to +20 mV from a $V_h$ of −60 mV (protocol shown at bottom) to inactivate $I_{K(V)}$. Reactivation of $I_{K(V)}$ was monitored upon the delayed application of a second step to +20 mV, 2 s in duration, from −60 mV. Only the membrane currents obtained after 0·5 s (first 3 pulses) and 2 s (last 9 pulses) incremental delays are shown for the sake of clarity. It is evident from this experiment that the recovery from inactivation of $I_{K(V)}$ was similar in the presence and absence of 4-AP.

Figure 4*D* shows a plot of the percentage recovery from inactivation of $I_{K(V)}$ as a function of time. Each data point is a mean ± S.E.M. of relative current (P2/P1 × 100) recorded at variable delays at −60 mV in control conditions (■) and after 0·5 mM 4-AP (□). The continuous and dashed lines are least-squares exponential fits to the mean data points. As reported by others, reactivation kinetics of $I_{K(V)}$ are extremely slow in vascular smooth muscle cells; for example, in the absence and presence of 4-AP, peak current had only partially recovered (87·3 ± 2·4 and 91·6 ± 2·1%, respectively) after an 18 s delay between control and test pulse. 4-Aminopyridine did not affect the time course of recovery from inactivation of $I_{K(V)}$ significantly.

**Block is reversed during step depolarizations**

The results of Fig. 2 suggested that the efficacy of 4-AP-induced block of $I_{K(V)}$ declined with membrane depolarization. Voltage-dependent unblock was also evident from examination of the recordings of Fig. 4*A*; the relative amount of block of $I_{K(V)}$ by 4-AP was greater at 0 mV than at +20 mV. Moreover, analysis of 4-AP-sensitive currents elicited during slow voltage ramps or long step protocols (5 s) also provided evidence consistent with the hypothesis of time-dependent unblock of 4-AP ('reverse use dependence') at positive potentials (Leblanc *et al.* 1994). We explored this possibility further by analysing the effects of 2 mM 4-AP on $I_{K(V)}$ evoked by short (250 ms) depolarizing steps from a $V_h$ of −70 mV (Fig. 5*A*, protocol at bottom). $I_{K(V)}$ was evoked using short steps in order to minimize time-dependent inactivation. Left and right families of traces in Fig. 5*A a* were obtained in control conditions and after block by 2 mM 4-AP, respectively. Figure 5*A b* shows the current–voltage relationship of the current measured at the end of the pulse for the families of current traces displayed in Fig. 5*A a*. As previously shown in Fig. 2, 4-AP inhibited $I_{K(V)}$ at all voltages. Figure 5*Ba* shows the

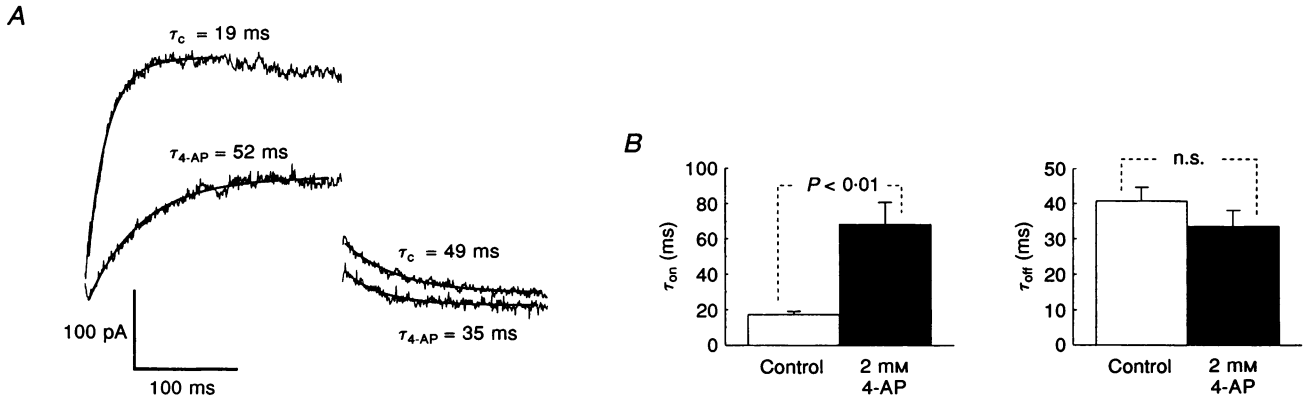


**Figure 3. Effects of 4-AP on the kinetics of activation and deactivation of $I_{K(V)}$**

*A*, representative current traces evoked by 250 ms steps to +20 mV from a $V_h$ of −60 mV in control conditions and after steady-state block by 2 mM 4-AP. The lines passing through the traces are monoexponential least-squares fits to the data for activation of $I_{K(V)}$ at +20 mV and current deactivation at −40 mV; the resulting time constants obtained for the controls ($\tau_c$) and 4-AP ($\tau_{4\text{-}AP}$) are illustrated. *B*, histograms summarizing the data obtained in 7 cells submitted to an identical voltage-clamp protocol to that described in *A*, in which activation (left histogram) and deactivation (right histogram) kinetics were analysed. For $\tau_{off}$, $P = 0{\cdot}076$. n.s., not significant.

difference currents obtained by digital subtraction of the two families of currents. Our data show that, in the range of −40 to −20 mV, 4-AP-sensitive currents activated in a time-dependent manner but exhibited little, if any, inactivation. However, at potentials positive to −20 mV, 4-AP-sensitive currents activated quickly but also displayed inactivation. While peak current continued to increase as a function of voltage, late current eventually

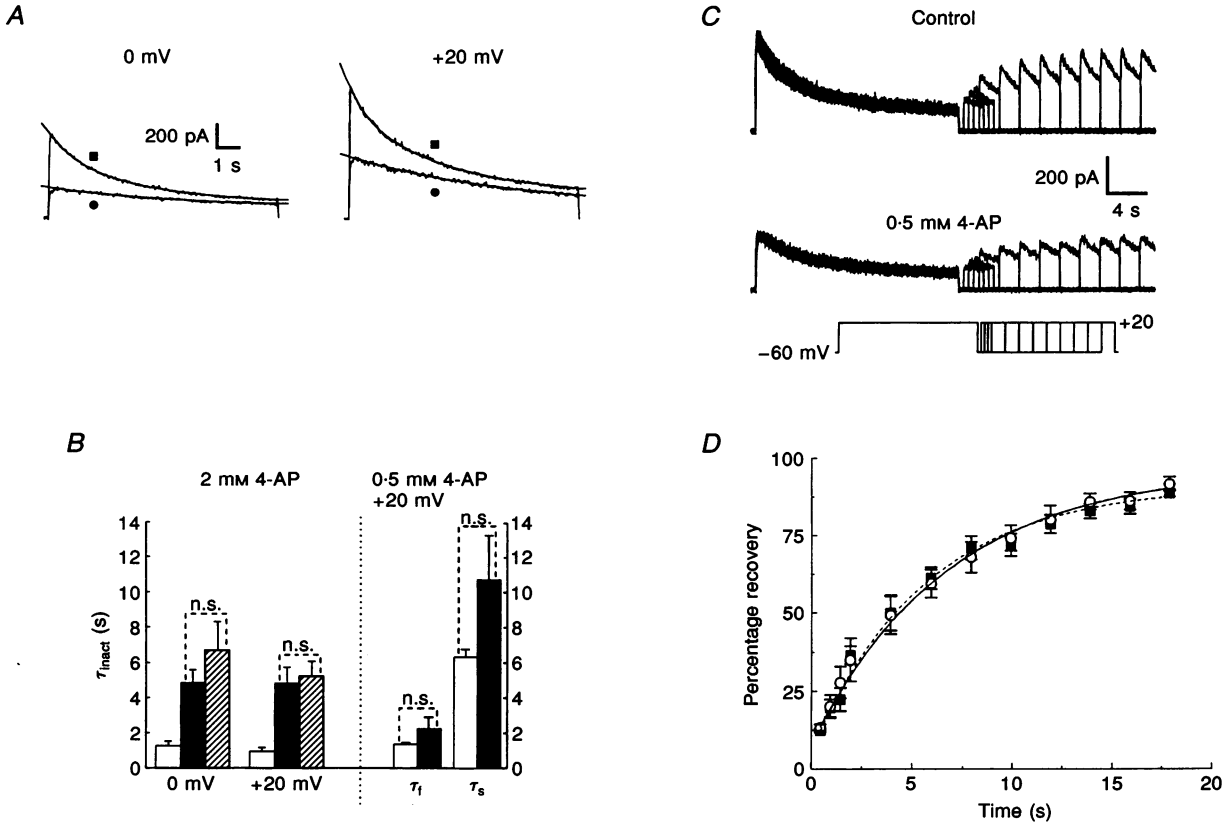


**Figure 4. Effects of 4-AP on the kinetics of inactivation of $I_{K(V)}$**

*A*, example of analysis of the effects of 4-AP on the kinetics of inactivation of $I_{K(V)}$ elicited by 10 s steps to either 0 (left traces) or +20 mV (right traces) from a $V_h$ of −60 mV. The thin lines superimposed on the current traces are least-squares double- and monoexponential fits for control (■) and 4-AP (●), respectively, at both voltages. *B*, histogram summarizing the inactivation kinetic data resulting from the analysis of the effects of 2 mM (left sets of bars; $N = 7$) and 0·5 mM (right sets of bars; $N = 4$) 4-AP. For 2 mM 4-AP: estimated means ± S.E.M. for fast ($\tau_f$) and slow ($\tau_s$) time constants of inactivation of $I_{K(V)}$ in control (□ and ■, respectively) are reported for measurements performed at 0 mV (left set of bars) and +20 mV (right set of bars). Only slow time constants could be estimated in the presence of 2 mM 4-AP (▨), values which were not significantly different from the slow time constant calculated for the control traces: 0 mV, $P = 0{\cdot}28$; +20 mV, $P = 0{\cdot}61$. At 0 mV, $\tau_f = 1{\cdot}2$ s and $\tau_s = 4{\cdot}6$ s in controls, and $\tau_s = 6{\cdot}1$ s in 4-AP. At +20 mV, $\tau_f = 0{\cdot}8$ s and $\tau_s = 4{\cdot}2$ s in controls, and $\tau_s = 7{\cdot}1$ s in 4-AP. For 0·5 mM 4-AP: fast and slow time constants of inactivation were estimated in controls (□) and in the presence of 0·5 mM 4-AP (■) at +20 mV; $\tau_f$ and $\tau_s$ were not significantly affected by 4-AP: $P = 0{\cdot}25$, $\tau_f$; $P = 0{\cdot}19$, $\tau_s$. n.s., not significant. *C*, a standard double-pulse protocol (shown at bottom) was used to estimate the recovery kinetics of $I_{K(V)}$ in the absence and presence of drug. Original recordings from a single cell in control conditions (top) and after steady-state block by 0·5 mM 4-AP (bottom). An initial constant 20 s pulse (P1) to +20 mV served to inactivate $I_{K(V)}$. This was followed by a second pulse (P2) to +20 mV (2 s in duration), which was imposed at incremental delays from a $V_h$ of −60 mV; interval between trains of pulses was 45 s. Reactivation of $I_{K(V)}$ was assessed by measuring the amplitude of $I_{K(V)}$ during P2 relative to that elicited by P1, and plotting the data as a function of time delay. *D*, plot of relative state of recovery from inactivation (%) as a function of time delay between P1 and P2 (see *C*). Each data point is a mean ± S.E.M. of relative current {(P2/P1) × 100} ($N = 4$). Points were fitted by a monoexponential function of the following form: $Y = \{Y_{max}[1 - \exp(-t/\tau_r)]\}$, where $t$ represents the time delay between the end of P1 and the onset of P2, and $\tau_r$ is the time constant of recovery from inactivation. The derived time constants were 5·7 and 6·8 s for controls (■, dashed line) and 0·5 mM 4-AP (○, continuous line), respectively. Mean values at each delay interval were not statistically different.

exhibited signs of saturation. Figure 5*Bb* shows the current–voltage relationship of the difference currents illustrated in Fig. 5*Ba* measured at the peak and at the end of the depolarizing step. The 4-AP-sensitive peak current increased from −30 to +60 mV and displayed slight inward rectification at potentials more positive than +20 mV. In contrast, the late current increased similarly between −30 and −10 mV but completely saturated at potentials $\geqslant 0$ mV. One possibility that explains the transient nature of 4-AP-sensitive currents is that the decaying phase reflects time-dependent unblock produced by transition to the open state. If unblock is purely state dependent, then the kinetics of unblock should be steeply voltage dependent within the activation voltage range. Figure 5*C* reports the voltage dependence of the time constant of the decaying phase of 4-AP-sensitive currents analysed by least-squares monoexponential fitting routines. The data points were fitted by a single exponential function, parameters of which are given in the figure legend. The data demonstrate a steep relationship between 0 and +20 mV, with little voltage dependence beyond that range. These data, together with those reported in Fig. 2, are consistent with the idea that the interaction of 4-AP with $K_V$ channels is state dependent.

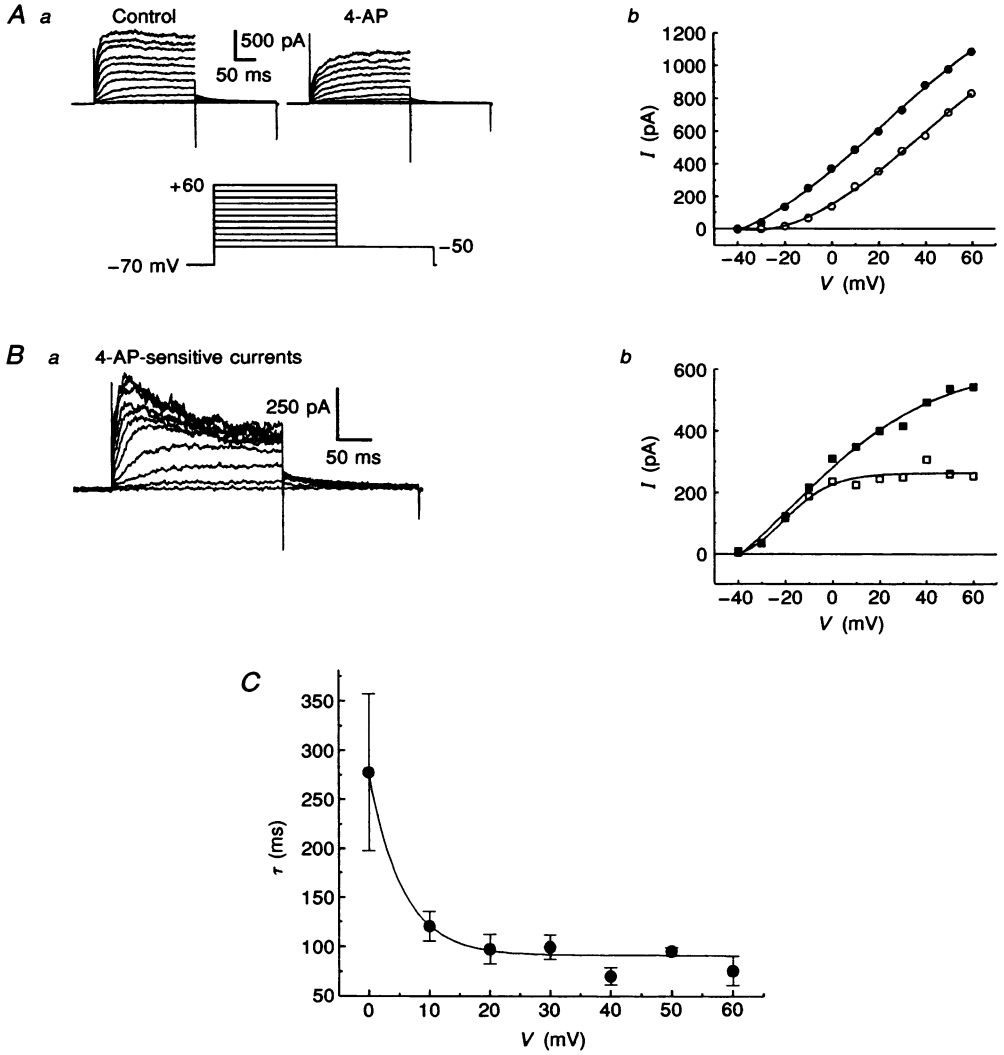


**Figure 5. Evidence for unblock of 4-AP during short step depolarizations**

*A*, from a $V_h$ of −70 mV, 250 ms depolarizing steps were applied in 10 mV increments according to the protocol shown at the bottom in order to evoke activation of $I_{K(V)}$ with little time-dependent inactivation of the current. *Aa*, traces in control conditions (left) and in 2 mM 4-AP (right). *Ab* shows *I–V* relationships of the current measured at the end of the pulse (late current) for the control (●) and 4-AP (○) current families displayed in *Aa*. *Ba* shows 4-AP-sensitive currents obtained by digital subtraction of the families of currents illustrated in *Aa*. Comparable results were obtained in 8 other myocytes. *Bb*, *I–V* relationships of peak (■) and late (□) difference currents depicted in *Ba*. *C*, voltage dependence of the time constant ($\tau$) of the decaying phase of 4-AP-sensitive currents at potentials more positive than −10 mV. Each data point is a mean ± S.E.M. ($N = 3$–9). The line passing through the data points is a weighted least-squares monoexponential fit with the following parameters: $\tau = \{185{\cdot}1\exp(-V/5{\cdot}49)\} + 91{\cdot}3$.

One possibility that explains these data is that the drug has greater affinity for binding the channel in the closed state. The apparent shifts of the steady-state activation and inactivation curves (Fig. 2), and slowing of the activation phase (Fig. 3), would also be consistent with this proposal. We therefore examined the effects of 4-AP on $I_{K(V)}$ evoked during trains of step depolarizations at a frequency of 0·25 Hz. Figure 6*A a* shows selected traces obtained in control conditions (top), in the presence of 0·5 mM 4-AP (middle) and after washout of 4-AP (bottom). Each train consisted of sixteen steps (250 ms) to +20 mV from a $V_h$ of −60 mV (protocol shown at bottom). Control traces were obtained after ~5 min of intracellular dialysis following whole-cell access. Traces in the presence of 0·5 mM 4-AP and after washout were obtained after 10 min incubation or washout of drug while the membrane potential was kept constant at −60 mV. In control conditions, the amplitude of the time-dependent current decreased slightly with the number of pulses (Fig. 6*A a* top, traces 1 and 12 are shown) following a monoexponential time course (Fig. 6*A b*, ■); this was probably produced by cumulative inactivation of $I_{K(V)}$ due to slow recovery kinetics (Fig. 4). In the presence of 4-AP, current amplitude changed little with the number of stimulations. There was no evidence of use-dependent block by the drug. In fact, the decline of current amplitude followed a linear time course, the rate of which was slower than in controls (Fig. 6*A b*, ●). During the first pulse of the train after washout, the current had only recovered by 24%. Resumption of stimulation quickly restored $I_{K(V)}$ to its pre-drug control level (Fig. 6*A a* bottom, traces 1 and 13 are shown; Fig. 6*A b*, ▲).

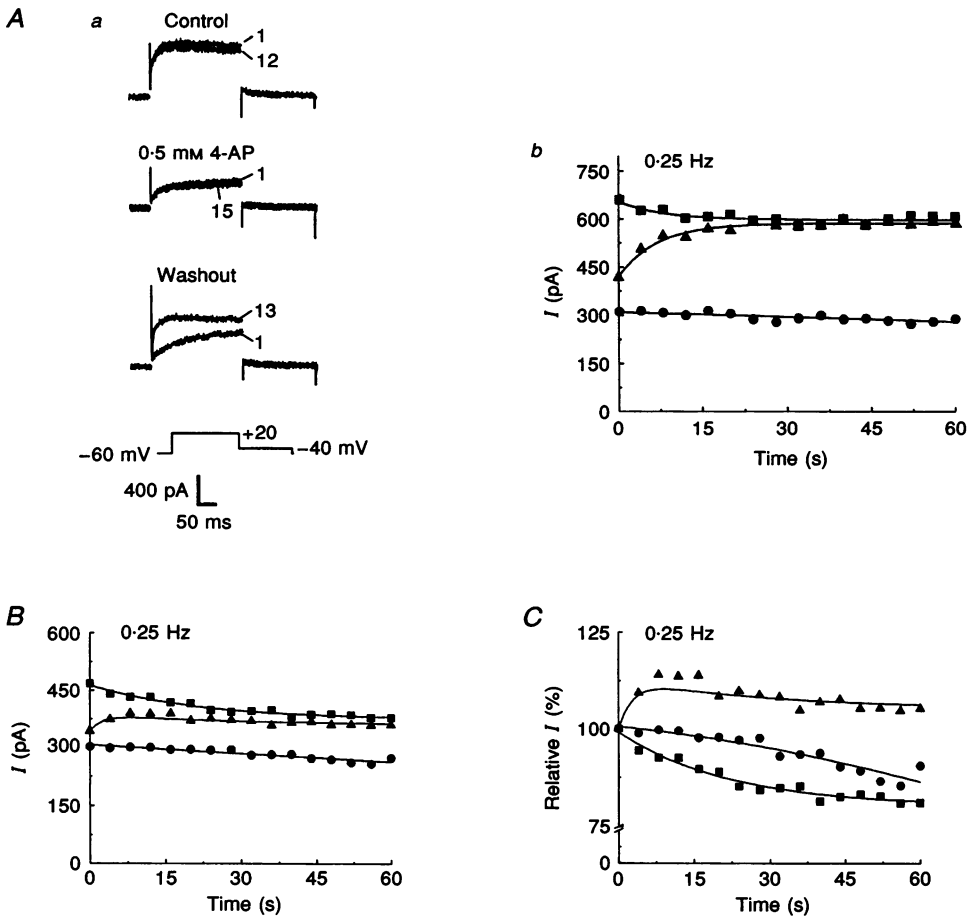


**Figure 6. Effects of repetitive depolarizations on 4-AP-induced block of $I_{K(V)}$**

*A*, response of $I_{K(V)}$ to trains of short (250 ms) depolarizing pulses applied at 4 s intervals (protocol shown at bottom). Shown are sample traces in control conditions (*A a*, top), following 10 min exposure to 4-AP (*A a*, middle) and after washout of the drug (*A a*, bottom), during which membrane potential was kept constant at −60 mV. Numbers next to the traces represent pulse number in the train for each condition; note that pulse 1 represents time zero. *A b* displays a plot of the time course of changes of $I_{K(V)}$ current measured at the end of the pulse in control conditions (■), with 0·5 mM 4-AP (●) and washout (▲) for the cell shown in *A a*. *B* and *C*, summarized data ($N = 5$) obtained for absolute current measurements (*B*) and relative currents (*C*). For *B*, S.E.M. ranged from ±108 to ±142 pA in controls, ±89 to ±112 pA in 4-AP and ±101 to ±119 pA following washout. For *C*, S.E.M. ranged from ±28 to ±31% in controls, ±34 to ±39% in 4-AP and ±28 to ±33% following washout. Symbols are identical to those in *A b*.

**Table 1. Parameters used to compute the mathematical model of the delayed rectifier $K^+$ current and its inhibition by 4-AP**

| | |
|---|---|
| Activation | |
| $\alpha_n(V) = 0{\cdot}117/\{1 + \exp[(-0{\cdot}1(V + 11{\cdot}9)]\}$ | ($ms^{-1}$) |
| $\beta_n(V) = 0{\cdot}251\exp[-0{\cdot}035(V + 99)]$ | ($ms^{-1}$) |
| Inactivation | |
| $\alpha_i(V) = 0{\cdot}387/\{1 + \exp[-0{\cdot}103(V + 21)]\}$ | ($s^{-1}$) |
| $\beta_i(V) = 0{\cdot}011\exp[-0{\cdot}0454(V + 51)]$ | ($s^{-1}$) |
| 4-AP binding and unbinding | |
| $\alpha_b(V) = \{(60/[91{\cdot}25 + (185{\cdot}1\exp(-0{\cdot}182V))] + 0{\cdot}0005)\}[4\text{-AP}]$ | ($mM^{-1}\ ms^{-1}$) |
| $\beta_b(V) = \{0{\cdot}02/[1 + (2{\cdot}03\exp(-0{\cdot}182V))]\} + 0{\cdot}000\,001$ | ($ms^{-1}$) |
| Conductance and selectivity | |
| $G_{K_V} = 0{\cdot}2$ mS $cm^{-2}$ at 22 °C | |
| $E_K = -83$ mV | |

$V$, voltage; $\alpha_x(V)$ and $\beta_x(V)$ are the functions expressing the voltage dependence (in mV) of the rate constants between the different states as described in the text; [4-AP], concentration of 4-aminopyridine; $G_{K_V}$, approximate maximum conductance of the $K_V$ channel (based on total cell capacitance and whole-cell current measurements taken from Leblanc *et al.* 1994); $E_K$, Nernst equilibrium potential for $K^+$, which was calculated based on the following equation: $E_K = RT/zF\log[K^+]_o/[K^+]_i$, where $[K^+]_o$ and $[K^+]_i$ were set to 5·4 and 140 mM, respectively.

Figure 6*B* and *C* shows the summarized data obtained in five myocytes for absolute current measurements (*B*) and relative currents (*C*) in control conditions (■), in 0·5 mM 4-AP (●) and after washout of the inhibitor (▲). Figure 6*C* confirms the suggestion of unblocking of 4-AP during the application of a series of depolarizing steps. Normalized outward currents were significantly larger after the first pulse in the presence of 4-AP *versus* control. In a separate set of experiments, normalized 4-AP currents (0·1 mM) were not significantly different from control currents when the frequency of stimulation was reduced from 0·25 to 0·1 Hz ($N = 3$; data not shown). These results further reinforce the idea that 4-AP preferentially blocks the $K_V$ channel in the closed state. Moreover, the washout experiments suggest that unbinding of the blocker is promoted by channel opening and that 4-AP remains trapped in a large fraction of the channels.

## Mathematical model of 4-AP-induced inhibition of $I_{K(V)}$

A simple formalism was used to reproduce mathematically the behaviour of macroscopic delayed rectifier $K^+$ current in rabbit coronary myocytes. Despite the fact that activation follows a sigmoidal time course in this preparation, this based on our own observations (data not shown), and the fact that whole-cell and ensembles of single-channel $I_{K(V)}$ were best fitted with the activation variable raised to the second power ($n^2$; Volk *et al.* 1991; Volk & Shibata, 1993), our main purpose was to construct a simplified model of the channel that would satisfactorily explain the interaction of 4-AP with the channel. For similar reasons, although the inactivation was best fitted by the sum of two exponential functions (Fig. 2*A* and *B*), fitting the inactivation with a single exponential relationship revealed only a slight deviation near peak current, which represented less than 5% of total current in all cells studied, suggesting that the slow component of inactivation represents the dominant transition from open to inactivated state. Consistent with this proposal was the fact that only the slow component of inactivation was reported by Volk & Shibata (1993) from the analysis of ensemble averages of single delayed rectifier $K^+$ channels recorded in the same preparation. The channel itself was therefore modelled as a simple three-state loop model incorporating single closed (C), open (O) and inactivated (I) states, as illustrated below. The kinetic model also shows that 4-AP was postulated to bind to the closed state, leading to a single non-conducting blocked state (B),

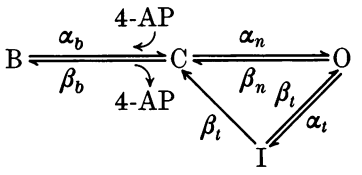


where $\alpha_x$ and $\beta_x$ represent, respectively, the forward and backward rate constants of the various transitions. The rate constants involved in channel activation were obtained by determining the time constants of activation and deactivation of $I_{K(V)}$ at different potentials elicited by step protocols similar to those described in Figs 2*A* and 3. Figure 7*A a* shows a plot of the voltage dependence of the time constants of activation (■) and deactivation (□). Both processes could be well fitted by single exponential functions. The bell-shaped voltage dependence of activation kinetics is similar to that reported by Volk *et al.* (1991) in the same preparation except that their values were about

3-fold larger than ours. Figure 7*A b* displays the voltage dependence of the rate constants, which were calculated according to the equations given in the inset, where $n_\infty$ is the level of steady-state activation (Fig. 2*B*) and $\tau$ the time constant (Fig. 7*A a*). The lines passing through the data points are Boltzmann and single exponential fits, which express the voltage dependence of both rate constants for incorporation into the model (Table 1).

A similar approach was used to derive the rate constants involved in the inactivation of $I_{K(V)}$. The graph in Fig. 7*B a* reports the voltage dependence of the time constant of inactivation (■), which was estimated from currents elicited during long step protocols similar to that described in Fig. 2*C*. A single point (□) is shown for the recovery from inactivation, which was taken from the experiments described in Fig. 4*D*. The time constants of Fig. 7*Ba* were used to obtain the rate constants at different potentials. Figure 7*Bb* shows a graph displaying the voltage dependence of the forward ($\alpha_t$) and backward ($\beta_t$) rate constants involved in the slow inactivation process; these parameters were calculated according to the equations

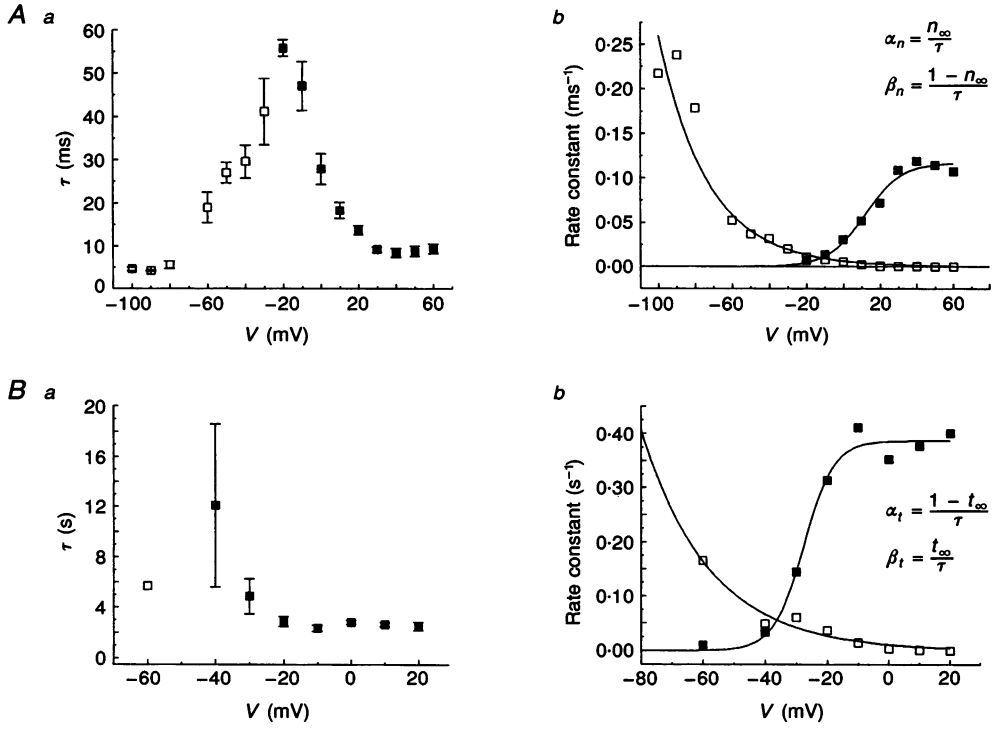


**Figure 7. Extraction of rate constants from estimated time constants of activation, deactivation, inactivation, and recovery from inactivation, for construction of a computer model of $I_{K(V)}$**

*A a*, voltage dependence of the time constants of activation ($\tau_{act}$, ■) and deactivation ($\tau_{deact}$, □). For activation, time constants were obtained from least-squares monoexponential fitting of time-dependent currents elicited in response to 250 ms steps from a $V_h$ of −60 mV (see Fig. 2*A*). Deactivation time constants were obtained from a similar analysis of tail current kinetics; from a $V_h$ of −60 mV, a constant 250 ms step to +20 mV (0·1 Hz) served to activate $I_{K(V)}$, followed by a second step from −100 to −30 mV (applied in 10 mV increments) to evoke tail current. Each data point is a mean ± S.E.M. of 3–7 measurements. *A b*, voltage dependence of the forward ($\alpha_n$, ■) and backward ($\beta_n$, □) rate constants, which were calculated according to the equations displayed on the graph (see text for explanations), where $\tau$ and $n_\infty$ represent, respectively, the time constants of activation or deactivation (*A a*) and relative state of activation (see Fig. 2*B*). The lines passing through the points are least-squares Boltzmann ($\alpha_n$) and monoexponential ($\beta_n$) fits, parameters of which are given in Table 1. *Ba*, voltage dependence of the time constants of inactivation ($\tau_{inact}$, ■) and recovery from inactivation ($\tau_{recov}$, □); these time constants were estimated from monoexponential fitting of currents evoked by protocols identical to those displayed in Figs 2*C* and 4*C* and *D*. For $\tau_{inact}$, each data point is a mean ± S.E.M. derived from 4–6 cells. For $\tau_r$, the single data point at −60 mV originated from the experiments described in Fig. 4*C* and *D*. *Bb*, voltage dependence of the forward ($\alpha_t$, ■) and backward ($\beta_t$, □) rate constants which were calculated according to the equations displayed on the graph (see text for explanations) where $\tau$ and $t_\infty$ represent, respectively, the time constants of inactivation or recovery from inactivation (*Ba*) and relative availability of $I_{K(V)}$ (see Fig. 2*D*). As for the activation gate, the lines passing through the points are least-squares Boltzmann ($\alpha_t$) and monoexponential ($\beta_t$) fits, parameters of which are given in Table 1.

given in Fig. 7*Bb*, where $t_\infty$ is the level of steady-state inactivation (Fig. 2*D*) and $\tau$ the time constant (Fig. 7*Ba*). The mathematical functions expressing the voltage dependence of both rate constants are included in Table 1.

The block by 4-AP was modelled as a state-dependent interaction, with 4-AP primarily binding to the closed state. The voltage dependence of the rate constants of association ($\alpha_b$) and dissociation ($\beta_b$) of 4-AP were derived from analysis of the voltage dependence of the time constant ($\tau$) of the decaying phase of the 4-AP-sensitive currents and based on the following equation:

$$\tau = 1/\{(\alpha_b[\text{4-AP}]) + \beta_b\}.$$

Binding of 4-AP was assumed to follow first-order rate reaction, with association being directly proportional to the concentration of 4-AP. Unbinding was assumed to be independent of the concentration of 4-AP (Castle & Slawsky, 1992). The amplitude of the sigmoidal voltage dependence of the binding and unbinding rate constants (data not shown) was adjusted to account for the experimentally observed changes in whole-cell current kinetics and voltage dependence of steady-state activation and inactivation. The functions expressing these relationships (Table 1) also comprised a constant term to account for binding and unbinding of 4-AP at negative voltages ($\sim < -50$ mV). These constants were obtained from analysis of the activation kinetics of $I_{K(V)}$ during trains of step depolarizations (Fig. 6; see also Fig. 9) and the amount of current recovery following washout (Fig. 6). The simple kinetic model presented above was resolved by the following system of first-order differential equations:

$$dC/dt = \beta_b B + \beta_n O + \beta_t I - C(\alpha_b + \alpha_n),$$
$$dB/dt = \alpha_b C[\text{4-AP}] - \beta_b B,$$
$$dO/dt = \alpha_n C + \beta_t I - O(\beta_n + \alpha_t),$$
$$dI/dt = \alpha_t O + \beta_t I,$$
$$O = 1 - (B + C + I),$$

where $\alpha_x$ and $\beta_x$ are the rate constants as defined above, and $B$, $C$, $O$ and $I$ represent the fraction of channels in the

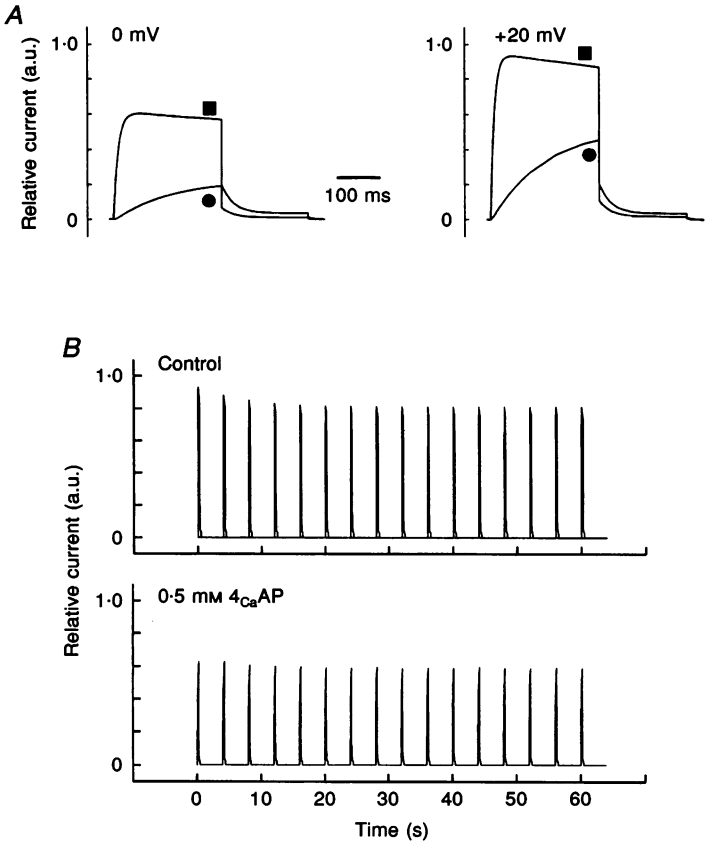


**Figure 8. Computer simulations of whole-cell $I_{K(V)}$ and its inhibition by 4-AP**

*A*, plotted on a relative scale (a.u., arbitrary units) are shown computer-generated control currents (■), and currents obtained following steady-state block by 2 mM 4-AP (●), at two different step potentials (250 ms in duration) as indicated. $V_h = -60$ mV; outward tail currents were elicited by repolarizing the membrane to −40 mV for 200 ms. *B*, reproduction by the computer model described in the text of the frequency dependence of $I_{K(V)}$ under control conditions (top graph) and after steady-state block by 0·5 mM 4-AP (bottom graph). The voltage-clamp protocol (250 ms steps to +20 mV (0·25 Hz), $V_h = -60$ mV) is identical to that used in actual experiments (Fig. 6).

blocked, closed, open and inactivated states, respectively. The last equation ensures conservation of the total number of channels.

Figure 8*A* illustrates the results of simulations carried out to examine the effects of 2 mM 4-AP on $I_{K(V)}$ elicited by 250 ms steps to 0 or +20 mV from a $V_h$ of −60 mV; tail currents were evoked by repolarizing the membrane to −40 mV. In the absence of drug, the model reproduced well the steady-state voltage dependence, kinetics and frequency-dependent changes of whole-cell $I_{K(V)}$ recorded in our preparation. As similarly observed in our experiments, the model was able to mimic the 4-AP-induced slowing of activation with little effect on deactivation kinetics, except for a small cross-over after ~6 s during long step depolarizing pulses (not shown). The model accounted well for the relative amount of block seen with this and other (Fig. 8*B*) concentrations of 4-AP, as well as the relatively greater degree of inhibition of $I_{K(V)}$ at more negative potentials (Figs 2*A*, 4*A* and 5*A a*), a result consistent with the observed positive shift of the activation curve (Fig. 2*B*).

Figure 8*B* illustrates the results of computer simulations designed to verify whether the model could account for the frequency-dependent effects of 4-AP in response to a train of stimulations. The protocol was identical to that of Fig. 6. The top and bottom graphs display simulated currents in control conditions and after steady-state block by 0·5 mM 4-AP. The model reproduced both the exponential decline of peak current seen in control conditions, which is related to slow recovery kinetics of $I_{K(V)}$, and the fact that the peak current remained relatively unchanged during the train of pulses (Fig. 6).

One reason for selecting a binding rate constant of 500 $M^{-1}$ $s^{-1}$ at −60 mV (see Table 1) came from the observation that the time constant of activation of $I_{K(V)}$ increased during the onset of the train after exposing the cell to 4-AP for 10 min while holding the membrane at −60 mV. Figure 9*A* shows a histogram of the estimated time constant ($\tau_{on}$) of activation at +20 mV of the first (P1) and second (P2) pulse of the train; the data were collected from the same series of experiments described in Fig. 6. As expected, there were no significant changes in $\tau_{on}$ for currents elicited during P1 and P2 in control conditions. In contrast, activation was significantly faster during P2 than P1 in the presence of 4-AP, but did not appreciably change during subsequent pulses (data not shown).

The computer model corroborated these observations. The top and middle graphs in Fig. 9*B* show simulated currents in control conditions and in the presence of 0·5 mM 4-AP during P1 and P2. Control currents displayed nearly identical activation phases; in contrast, the current elicited by P2 displayed a faster onset than that triggered by P1 with 4-AP, consistent with the data presented in Fig. 9*A*.

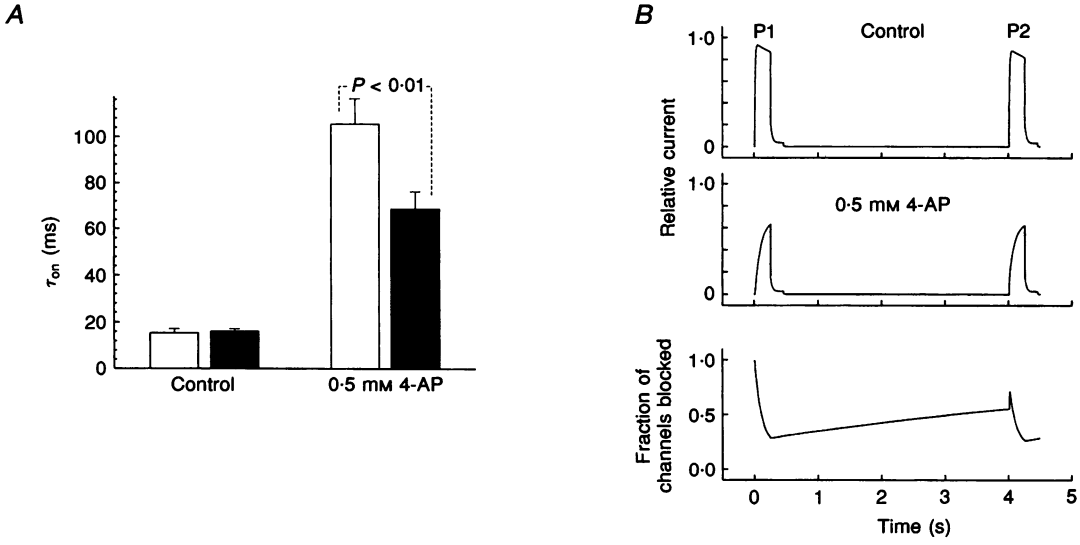


**Figure 9. Evidence for unblocking of 4-AP during a train of depolarizing pulses provided by analysis of activation kinetics**

*A*, time constants of activation ($\tau_{on}$) of the first (P1, □) and second (P2, ■) pulses of a train of depolarizing steps to +20 mV from a $V_h$ of −60 mV (0·25 Hz) in control conditions (left set of bars) and after steady-state inhibition by 0·5 mM 4-AP (right set of bars). These data were derived from the same experiments described in Fig. 6. Each bar is a mean ± S.E.M. ($N = 4$). *B*, on a relative scale are displayed computer-generated whole-cell currents in control conditions (top graph) and in the presence of 0·5 mM 4-AP (middle graph) in response to an identical voltage-clamp protocol to that of Fig. 6, which was designed to examine the frequency dependence of $I_{K(V)}$ in the absence and presence of drug. The bottom graph displays a plot of the time course of changes of the fraction of blocked channels following initiation of stimulation.

The bottom graph reports the time-dependent changes in the fraction of blocked channels during the 4-AP simulation (middle graph). At the start of the simulation, nearly all channels would be blocked by 4-AP. During P1, the fraction of blocked channels would rapidly decline due to state-dependent unbinding of 4-AP. Following repolarization to −40 mV (200 ms) and then to −60 mV (3·55 s), 4-AP would slowly reassociate to channels in the closed state. However, before the onset of P2, ~50% of channels would still be in the closed state and readily available for opening. A consequence of this would be acceleration of the activation phase of the whole-cell current.

## DISCUSSION

Our data show that block of the delayed rectifier $K^+$ current in rabbit coronary myocytes by 4-aminopyridine is state dependent, with 4-AP primarily inhibiting the channels in the closed state. This conclusion is based on the following observations: (i) under steady-state blocking conditions, 4-AP slowed activation kinetics but had little influence on the time course of deactivation; (ii) block developed fully in the absence of stimulations while holding the cells at negative holding potentials; and (iii) inhibition of $I_{K(V)}$ by 4-AP was not promoted by repetitive depolarizations after resting block was complete; in contrast, opening of the channels evoked by depolarization slightly relieved the 4-AP-induced block of $I_{K(V)}$, a process described as 'reverse use dependence'. Our experiments also suggested that 4-AP is more tightly bound to the channel at negative voltages (closed or resting state block), and the block may be quickly relieved by opening of the channels at positive potentials.

### Potency of block by 4-AP in rabbit coronary myocytes

Estimation of half-maximal inhibition of $I_{K(V)}$ by 4-AP revealed that the compound inhibits these channels with relatively low affinity. The $K_{½}$ value reported here (1·37 mM) is at the top end of the range of values obtained in other smooth muscle cells. $K_{½}$ values of 0·3 and 0·723 mM have been estimated in rabbit pulmonary artery (Okabe *et al.* 1987) and canine renal artery (Gelband & Hume, 1992) cells, respectively. In our experiments, application of 4-AP resulted in 81% block of $I_{K(V)}$, which is very similar to that reported by Volk *et al.* (1991), who documented 74% block at +10 mV with the same concentration of 4-AP. This supports the notion that the reported efficacy of inhibition of $I_{K(V)}$ by 4-AP in our preparation is not the result of differences in experimental conditions or cell dispersion technique but truly reflects the interaction of 4-AP with $K_V$ channels in this species.

However, one must be careful in interpreting the $K_{½}$ value in terms of kinetics of binding of 4-AP to the channel. Although it does reflect the concentration of 4-AP producing half-maximal inhibition of peak current, it cannot be used to estimate the rate constants of association and dissociation (where $K_{½} = k_{off}/k_{on}$) because: (i) the block is highly voltage dependent, with declining potency as the membrane is depolarized; and (ii) around peak, some channels are still unblocking, so that the potency of block is estimated under non-steady-state conditions; in this context, if $K_V$ channels were not inactivating, the concentration of 4-AP producing half-maximal inhibition would probably be higher than the value reported in this study.

### Nature of the 4-AP-sensitive current

Proper current isolation was essential for analysing the mechanism of block induced by 4-AP. Our data support the idea that $I_{K(V)}$ recorded in our experiments largely reflects the behaviour of delayed rectifier $K^+$ channels with little contamination by other time-dependent ionic currents. This is based on the following observations. (i) L-type $Ca^{2+}$ channels were inhibited by an effective dose of nifedipine (Leblanc *et al.* 1994). (ii) The activity of $K_{Ca}$ and $Cl_{Ca}$ channels was minimized by buffering intracellular $Ca^{2+}$ with EGTA; in addition, in most experiments, the superfusate also contained 0·5 mM TEA to inhibit $K_{Ca}$ channels (Leblanc *et al.* 1994). (iii) ATP (1 mM) was included in the pipette solution to minimize the activity of $K_{ATP}$ channels; it is unlikely that these channels would have interfered with our measurements since they are time independent (Clapp & Gurney, 1992). (iv) Besides the sigmoidal onset during depolarizing steps, both activation and deactivation phases of $I_{K(V)}$ could be well fitted by single exponential functions at all voltages examined, which is inconsistent with the existence of a distinct $K^+$ channel unless its kinetics are identical to those of $I_{K(V)}$. It is unlikely that these currents would correspond to the voltage-dependent fast transient outward current ($I_{fo}$ or $I_{to}$; '$I_A$-like') reported in rabbit portal vein (Beech & Bolton, 1989*a*) and colonic (Vogalis & Lang, 1994) smooth muscle cells. These currents activate and inactivate at more negative potentials and display faster inactivation kinetics. Distinct components of time- and voltage-dependent delayed rectifier $K^+$ channels have been identified in dog colonic myocytes (Carl, 1995). Although the pharmacological profile of these components was clearly different from that of $I_{K(V)}$ in coronary myocytes (use- and voltage-dependence of block by 4-AP), we cannot rule out the possibility that several populations of $K_V$ channels also exist in our preparation, even though a single component of delayed rectifier $K^+$ channels has been documented at the whole-cell (Volk *et al.* 1991; Leblanc *et al.* 1994) and single-channel (Volk & Shibata, 1993) levels in the same preparation, and which shared many characteristics with those reported for tracheal (Boyle *et al.* 1992; Fleischmann *et al.* 1993), portal vein (Hume & Leblanc, 1989; Beech &

Bolton, 1989*a*,*b*; Miller *et al.* 1993), renal (Gelband & Hume, 1992), cerebral (Brayden & Nelson, 1992; Robertson & Nelson, 1994) and pulmonary arterial (Okabe *et al.* 1987; Clapp & Gurney, 1992; Smirnov *et al.* 1994; Yuan *et al.* 1994) smooth muscle cells. The different sensitivity of the fast inactivation component to 0·5 and 2 mM 4-AP could be an indication that $I_{K(V)}$ reflects the activity of at least two components. However, even if this is the case, it would not compromise our major conclusions because the fast inactivation component represented less than 10% of total current (based on extrapolation of exponential fits to time zero) at potentials more positive than 0 mV, and was not apparent at potentials below that level. Moreover, although $\tau_f$ was unaffected by 0·5 mM 4-AP, the estimated amplitude of the fast component decreased and paralleled the changes of the slow component.

### State-dependent inhibition of $I_{K(V)}$

Previous studies suggested that the 4-AP-induced block of delayed rectifier $K^+$ channels is voltage dependent with diminished efficacy of the compound at depolarized membrane potentials (Okabe *et al.* 1987; Volk *et al.* 1991; Leblanc *et al.* 1994). Our data and computer simulations support the view that 4-AP preferentially interacts with rabbit coronary smooth muscle $K_V$ channels when they are in the closed state, while membrane depolarization relieves the inhibition through a state-dependent mechanism. The following observations were consistent with this proposal: (i) 4-AP delayed the onset of activation of $I_{K(V)}$; deactivation and inactivation kinetics were little affected; (ii) 4-AP shifted the steady-state activation curve toward positive potentials and steepened the relationship; (iii) block developed fully while the channels were kept in the closed state with the use of negative holding potentials, and was partially alleviated by a train of depolarizing pulses, a phenomenon commonly referred to as 'reverse use dependence'; and (iv) a simple four-state mathematical model involving voltage-dependent kinetics of interaction of 4-AP with the closed state reproduced both the features of the control whole-cell $I_{K(V)}$ and its inhibition by the blocker. The behaviour of $I_{K(V)}$ in the presence of 4-AP was similar to that reported for the delayed rectifier $K^+$ current in squid axon (Yeh, Oxford, Wu & Narahashi, 1976; Kirsch, Yeh & Oxford, 1986), and for the rapidly inactivating transient outward $K^+$ current ($I_{to}$) in ventricular myocytes (Šimurda, Šimurdová & Christé, 1989; Castle & Slawsky, 1992; Campbell, Qu, Rasmusson & Strauss, 1993; Jahnel, Klemm & Nawrath, 1994) and melanotroph cells (Kehl, 1990). In squid axon (Kirsch *et al.* 1986) and ventricular myocytes (Castle & Slawsky, 1992; Campbell *et al.* 1993), the concentration and voltage dependence of block by 4-AP was explained by assuming that the sequential closed states through which the channel passes during activation would exhibit successively lower affinity toward 4-AP, thus leading to time-dependent unblocking.

As reported in the above studies, our data and theoretical simulations were more consistent with a state-dependent mechanism than with a purely voltage-dependent interaction whereby 4-AP binding would depend on the transmembrane electric field. In addition to the observed positive displacements of the steady-state activation and inactivation curves, analysis of the voltage dependence of the time constant of the decaying phase of 4-AP-sensitive currents demonstrated a steep relationship within the activation range of $I_{K(V)}$, with little dependency at potentials more positive than +10 mV. Computer simulations based on this model were able to reproduce the data reasonably well. To account for the changes in kinetics, voltage dependence and frequency-dependent changes of $I_{K(V)}$ during a train of pulses, both the binding and unbinding rate constants had to be increased in a sigmoidal fashion as a function of voltage (see Table 1); however, the ratio of the unbinding to the binding rate constants increased ~15-fold with 2 mM 4-AP from −60 to +20 mV. Unblocking of $K_V$ channels at positive potentials would result from both the increased ratio of unbinding to binding rates, and the fact that the channels that did unblock would be subsequently available for either a transition to the open state, or for reassociation with 4-AP as driven by the law of mass action.

The features of 4-AP-induced inhibition of rabbit coronary $I_{K(V)}$ appear inconsistent with a mechanism that would require channel opening for 4-AP to reach its binding site. Open state block by 4-AP has been reported for voltage-gated $K^+$ channels in lymphocytes (Choquet & Korn, 1992), dorsal root ganglia neurons (Ogata & Tatebayashi, 1993), and expressed non- or slowly inactivating $K^+$ channel clones from the *Drosophila shaker* ($K_V1.1$: Stephens, Garratt, Robertson & Owen, 1994; $K_V1.2$: Russell *et al.* 1994*b*; $K_V1.4$: Yao & Tseng, 1994), *shab* ($K_V2.1$) and *shaw* ($K_V3.1$) subfamilies (Kirsch & Drewe, 1993), which required channel opening for onset of block, and displayed use-dependent inhibition. Although we did not observe acceleration of current decay during the first and second pulse of a train protocol, as typically reported for $K^+$ channels exhibiting open state block, we cannot rule out the possibility that 4-AP may interact with channels open at negative holding potentials due to a small but significant open probability. However, such a mechanism would be difficult to reconcile with the observed slowing of activation of $I_{K(V)}$ and its response during a train of depolarizing stimuli, unless channels that bind to 4-AP in the open state (open-bound state, which would be non-conducting) could undergo a conformational change to a closed-bound state, which would tightly retain or trap the molecule. The trapping phenomenon has been suggested for certain $K^+$ channels that exhibited typical open state block by 4-AP (Choquet & Korn, 1992; Castle, Fadous, Logothetis & Wang, 1994). In our experiments, the trapping of 4-AP by $K_V$ channels in

the closed state, and its rapid release by membrane depolarization, could be reproduced well by our computer model, which assumed an extremely slow dissociation constant of 4-AP at negative potentials ($0{\cdot}001\ s^{-1}$), and rapid unblocking due to state-dependent unbinding. The exact mechanism will require further investigation at the single-channel level.

At a concentration of 0·5 mM, 4-AP produced little, if any, effect on inactivation kinetics and recovery from inactivation, supporting the view that it probably did not interfere *per se* with the inactivation gating mechanisms. Although we do not have an explanation for the disappearance of the fast time constant of inactivation with 2 mM 4-AP, one possibility may be that, since the fast component of inactivation represents a small fraction of total current, a higher concentration of 4-AP could result in a lower probability of finding channels undergoing a transition to rapid inactivation. This effect would be accentuated by a 4-AP-induced concentration-dependent shift of the steady-state activation relationship of $I_{K(V)}$. Another argument would be that, as discussed above, it is also possible that the fast and slow components represent two distinct populations of $K_V$ channels (Carl, 1995) displaying different sensitivities to 4-AP. Another explanation may be that, at higher concentration, 4-AP is competing for a common binding site with an endogenous $\beta$-subunit particle involved in rapid inactivation of $I_{K(V)}$, as recently demonstrated for selected members of the $K_V1$ subfamily of voltage-gated $K^+$ channels (Rettig *et al.* 1994). Nevertheless, our results are consistent with previous studies on various potassium channels, which concluded that 4-AP mainly interacts with the channels with their inactivation gate open, regardless of whether it involves a closed (Šimurda *et al.* 1989; Kehl, 1990; Castle & Slawsky, 1992; Campbell *et al.* 1993) or open state interaction (Yao & Tseng, 1994; Russell *et al.* 1994*b*), or both (Thompson, 1982). Moreover, the potency of block by 4-AP was promoted by deletion through site-directed mutagenesis of a peptide segment responsible for the fast inactivation gate of the $K_V1.4$ clone, suggesting that 4-AP binding and inactivation are mutually exclusive. Consistent with the latter was the observation that, in coronary smooth muscle cells, 2 mM 4-AP induced a +16 mV shift of the steady-state inactivation curve of $I_{K(V)}$, a finding similar to that reported by others (Thompson, 1982; Kehl, 1990; Ogata & Tatebayashi, 1993). Our computer model, which is based on a closed state interaction, predicted a concentration-dependent shift of the availability curve, as observed by Castle & Slawsky (1992) for $I_{to}$ in rat ventricular myocytes; half-maximal steady-state inactivation was shifted from a control value of −32 mV by +9, +13 and +14 mV with 0·5, 2 and 10 mM 4-AP, respectively. Interaction of 4-AP with the inactivation gate has, however, been proposed for inactivating $K^+$ currents in lymphocytes (Choquet & Korn, 1992).

**Physiological significance of our findings**

Our data support the notion that delayed rectifier $K^+$ channels of coronary myocytes represent a family of channels that is distinct from the $K_V1.2$ recently cloned from colonic smooth muscle and expressed in *Xenopus* oocytes, which exhibited strict open state block by 4-AP (Russell *et al.* 1994*b*) with a $K_{½}$ of 74·4 μM (Hart *et al.* 1993). The above considerations are consistent with the recent demonstration that $K_V1.2$ is almost exclusively expressed in gastrointestinal smooth muscles (Overturf *et al.* 1994). A $K^+$ channel homologous to the $K_V1.5$ subtype was recently cloned from colonic circular smooth muscle and shown to be uniformly expressed in vascular, visceral and uterine smooth muscles (Overturf *et al.* 1994). The properties of this channel differed somewhat from that reported here with a $K_{½}$ of 211 μM. Our group also recently reported that rabbit coronary $I_{K(V)}$ is sensitive to charybdotoxin at concentrations of 50 and 100 nM (Leblanc *et al.* 1994) whereas visceral smooth muscle $K_V1.5$ is insensitive to this toxin at concentrations up to 300 nM (Russell, Overturf & Horowitz, 1994*a*). On the other hand, we cannot rule out the possibility that $I_{K(V)}$ results from the assembly of a heterotetrameric structure involving varied proportions of monomers of different $K^+$ channel subtypes (Russell *et al.* 1994*a*).

In conclusion, our data suggest that 4-aminopyridine inhibits delayed rectifier $K^+$ channels in rabbit coronary myocytes by preferentially interacting with the channels in the closed state. Inhibition is alleviated by membrane depolarization due to a state-dependent unblocking process that is concurrent to the activation gating mechanism. 4-Aminopyridine depolarizes smooth muscle cells (Okabe *et al.* 1987; Gelband & Hume, 1992; Post *et al.* 1992; Miller *et al.* 1993; Fleischmann *et al.* 1993; Leblanc *et al.* 1994; Smirnov *et al.* 1994; Robertson & Nelson, 1994; Yuan *et al.* 1994) by inducing a positive displacement of the steady-state activation curve of $I_{K(V)}$. Rapid unbinding of 4-AP during depolarization warrants caution in assessing the absolute and relative contributions of delayed rectifier $K^+$ channels in determining the resting membrane potential and total macroscopic currents at potentials more positive than −20 mV.

Beech, D. J. & Bolton, T. B. (1989*a*). A voltage-dependent outward current with fast kinetics in single smooth muscle cells isolated from rabbit portal vein. *Journal of Physiology* **412**, 397–414.

Beech, D. J. & Bolton, T. B. (1989*b*). Two components of potassium current activated by depolarization of single smooth muscle cells from the rabbit portal vein. *Journal of Physiology* **418**, 293–309.

Boyle, J. P., Tomasic, M. & Kotlikoff, M. I. (1992). Delayed rectifier potassium channels in canine and porcine airway smooth muscle cells. *Journal of Physiology* **447**, 329–350.

Brayden, J. E. & Nelson, M. T. (1992). Regulation of arterial tone by activation of calcium-dependent potassium channels. *Science* **256**, 532–535.

CAMPBELL, D. L., QU, Y., RASMUSSON, R. L. & STRAUSS, H. C. (1993). The calcium-independent transient outward potassium current in isolated ferret right ventricular myocytes. *Journal of General Physiology* **101**, 603–626.

CARL, A. (1995). Multiple components of delayed rectifier $K^+$ current in canine colonic smooth muscle. *Journal of Physiology* **484**, 339–353.

CASTLE, N. A., FADOUS, S., LOGOTHETIS, D. E. & WANG, G. K. (1994). Aminopyridine block of $K_v1.1$ potassium channels expressed in mammalian cells and *Xenopus* oocytes. *Molecular Pharmacology* **45**, 1242–1252.

CASTLE, N. A. & SLAWSKY, M. T. (1992). Characterization of 4-aminopyridine block of the transient outward $K^+$ current in adult rat ventricular myocytes. *Journal of Pharmacology and Experimental Therapeutics* **264**, 1450–1459.

CHOQUET, D. & KORN, H. (1992). Mechanism of 4-aminopyridine action on voltage-gated potassium channels in lymphocytes. *Journal of General Physiology* **99**, 217–240.

CLAPP, L. H. & GURNEY, A. M. (1992). ATP-sensitive $K^+$ channels regulate resting potential of pulmonary arterial smooth muscle cells. *American Journal of Physiology* **262**, H916–920.

FLEISCHMANN, B. K., WASHABAU, R. J. & KOTLIKOFF, M. I. (1993). Control of resting membrane potential by delayed rectifier potassium currents in ferret airway smooth muscle cells. *Journal of Physiology* **469**, 625–638.

GELBAND, C. H. & HUME, J. R. (1992). Ionic currents in single smooth muscle cells of the canine renal artery. *Circulation Research* **71**, 745–758.

HAMILL, O. P., MARTY, A., NEHER, E., SAKMANN, B. & SIGWORTH, F. J. (1981). Improved patch-clamp techniques for high-resolution current recording from cells and cell-free membrane patches. *Pflügers Archiv* **391**, 85–100.

HART, P. J., OVERTURF, K. E., RUSSELL, S. N., CARL, A., HUME, J. R., SANDERS, K. M. & HOROWITZ, B. (1993). Cloning and expression of a $K_v1.2$ class delayed rectifier $K^+$ channel from canine colonic smooth muscle. *Proceedings of the National Academy of Sciences of the USA* **90**, 9659–9663.

HUME, J. R. & LEBLANC, N. (1989). Macroscopic $K^+$ currents in single smooth muscle cells of the rabbit portal vein. *Journal of Physiology* **413**, 49–73.

JAHNEL, U., KLEMM, P. & NAWRATH, H. (1994). Different mechanisms of the inhibition of the transient outward current in rat ventricular myocytes. *Naunyn-Schmiedeberg's Archives of Pharmacology* **349**, 87–94.

KEHL, S. J. (1990). 4-Aminopyridine causes a voltage-dependent block of the transient outward $K^+$ current in rat melanotrophs. *Journal of Physiology* **431**, 515–528.

KIRSCH, G. E. & DREWE, J. A. (1993). Gating-dependent mechanism of 4-aminopyridine block in two related potassium channels. *Journal of General Physiology* **102**, 797–816.

KIRSCH, G. E., YEH, J. Z. & OXFORD, G. S. (1986). Modulation of aminopyridine block of potassium currents in squid axon. *Biophysical Journal* **50**, 637–644.

LEBLANC, N., WAN, X. & LEUNG, P. M. (1994). Physiological role of $Ca^{2+}$-activated and voltage-dependent $K^+$ currents in rabbit coronary myocytes. *American Journal of Physiology* **266**, C1523–1537.

MILLER, A. L., MORALES, E., LEBLANC, N. R. & COLE, W. C. (1993). Metabolic inhibition enhances $Ca^{2+}$-activated $K^+$ current in smooth muscle cells of rabbit portal vein. *American Journal of Physiology* **265**, H2184–2195.

OGATA, N. & TATEBAYASHI, H. (1993). Differential inhibition of a transient $K^+$ current by chlorpromazine and 4-aminopyridine in neurones of the rat dorsal root ganglia. *British Journal of Pharmacology* **109**, 1239–1246.

OKABE, K., KITAMURA, K. & KURIYAMA, H. (1987). Features of 4-aminopyridine sensitive outward current observed in single smooth muscle cells from the rabbit pulmonary artery. *Pflügers Archiv* **409**, 561–568.

OVERTURF, K. E., RUSSELL, S. N., CARL, A., VOGALIS, F., HART, P. J., HUME, J. R., SANDERS, K. M. & HOROWITZ, B. (1994). Cloning and characterization of a $K_v1.5$ delayed rectifier $K^+$ channel from vascular and visceral smooth muscles. *American Journal of Physiology* **262**, C1231–1238.

POST, J. M., HUME, J. R., ARCHER, S. L. & WEIR, E. K. (1992). Direct role for potassium channel inhibition in hypoxic pulmonary vasoconstriction. *American Journal of Physiology* **262**, C882–890.

REMILLARD, C. V. & LEBLANC, N. (1995). Voltage- and state-dependent block of delayed rectifier $K^+$ current by 4-aminopyridine in rabbit coronary smooth muscle cells. *Biophysical Journal* **68**, A38.

RETTIG, J., HEINEMANN, S. H., WUNDER, F., LORRA, C., PARCEJ, D. N., DOLLY, J. O. & PONGS, O. (1994). Inactivation properties of voltage-gated $K^+$ channels altered by presence of beta-subunit. *Nature* **369**, 289–294.

ROBERTSON, B. E. & NELSON, M. T. (1994). Aminopyridine inhibition and voltage dependence of $K^+$ currents in smooth muscle cells from cerebral arteries. *American Journal of Physiology* **267**, C1589–1597.

RUSSELL, S. N., OVERTURF, K. E. & HOROWITZ, B. (1994*a*). Heterotetramer formation and charybdotoxin sensitivity of two $K^+$ channels cloned from smooth muscle. *American Journal of Physiology* **267**, C1729–1733.

RUSSELL, S. N., PUBLICOVER, N. G., HART, P. J., CARL, A., HUME, J. R., SANDERS, K. M. & HOROWITZ, B. (1994*b*). Block by 4-aminopyridine of a $K_v1{\cdot}2$ delayed rectifier $K^+$ current expressed in *Xenopus* oocytes. *Journal of Physiology* **481**, 571–584.

ŠIMURDA, J., ŠIMURDOVÁ, M. & CHRISTÉ, G. (1989). Use-dependent effects of 4-aminopyridine on transient outward currents in dog ventricular muscle. *Pflügers Archiv* **415**, 244–246.

SMIRNOV, S. V., ROBERTSON, T. P., WARD, J. P. T. & AARONSON, P. I. (1994). Chronic hypoxia is associated with reduced delayed rectifier $K^+$ current in rat pulmonary artery muscle cells. *American Journal of Physiology* **266**, H365–370.

STEPHENS, G. J., GARRATT, J. C., ROBERTSON, B. & OWEN, D. G. (1994). On the mechanism of 4-aminopyridine action on the cloned mouse brain potassium channel mKv1.1. *Journal of Physiology* **477**, 187–196.

THOMPSON, S. (1982). Aminopyridine block of transient potassium current. *Journal of General Physiology* **80**, 1–18.

VOGALIS, F. & LANG, R. J. (1994). Identification of single transiently opening ("A-type") K channels in rabbit coronary artery smooth muscle cells. *Pflügers Archiv* **429**, 160–164.

VOLK, K. A., MATSUDA, J. J. & SHIBATA, E. F. (1991). A voltage-dependent potassium current in rabbit coronary artery smooth muscle cells. *Journal of Physiology* **439**, 751–768.

VOLK, K. A. & SHIBATA, E. F. (1993). Single delayed rectifier potassium channels from rabbit coronary artery myocytes. *American Journal of Physiology* **264**, H1146–1153.

YAO, J. A. & TSENG, G. N. (1994). Modulation of 4-AP block of a mammalian A-type K channel clone by channel gating and membrane voltage. *Biophysical Journal* **67**, 130–142.

YEH, J. Z., OXFORD, G. S., WU, C. H. & NARAHASHI, T. (1976). Dynamics of aminopyridine block of potassium channels in squid axon membrane. *Journal of General Physiology* **68**, 519–535.

YUAN, X. J., TOD, M. L., RUBIN, L. J. & BLAUSTEIN, M. P. (1994). Deoxyglucose and reduced glutathione mimic effects of hypoxia on $K^+$ and $Ca^{2+}$ conductances in pulmonary artery cells. *American Journal of Physiology* **267**, L52–63.

**Acknowledgements**

We are grateful to Marie-Andrée Lupien for isolating single smooth muscle cells. This work was supported by an operating grant from the Medical Research Council (MRC) of Canada. C.V.R. is a pre-doctoral fellow of the Heart and Stroke Foundation of Canada (HSFC). N.L. is a MRC Scholar of Canada.

*Received 24 March 1995; accepted 13 September 1995.*